Physics Letters B 703 (2011) 417–421

Contents lists available at ScienceDirect

Physics Letters B

www.elsevier.com/locate/physletb

Spectroscopy of ^{39,41}Si and the border of the $N = 28$ island of inversion

D. Sohler [a,*], S. Grévy [b,c], Zs. Dombrádi [a], O. Sorlin [b], L. Gaudefroy [d], B. Bastin [b], N.L. Achouri [e], J.C. Angélique [e], F. Azaiez [f], D. Baiborodin [g], R. Borcea [h], C. Bourgeois [f], A. Buta [h], A. Burger [i,j], L. Caceres [b], R. Chapman [k], J.C. Dalouzy [b], Z. Dlouhy [g], A. Drouard [i], Z. Elekes [a], S. Franchoo [f], S. Iacob [h], I. Kuti [a], B. Laurent [e], M. Lazar [h], X. Liang [k], E. Liénard [e], S.M. Lukyanov [l], J. Mrazek [g], L. Nalpas [i], F. Negoita [h], F. Nowacki [m], N.A. Orr [e], Yu.E. Penionzkhevitch [l], Zs. Podolyák [n], F. Pougheon [f], A. Poves [o], P. Roussel-Chomaz [b], M. Stanoiu [h], I. Stefan [f], M.G. St-Laurent [b]

[a] *Institute of Nuclear Research, H-4001 Debrecen, Pf. 51, Hungary*
[b] *GANIL, CEA/DSM-CNRS/IN2P3, BP 55027, F-14076 Caen Cedex 5, France*
[c] *Centres d'Etudes Nucléaires de Bordeaux Gradignan, Université Bordeaux 1, UMR 5797 CNRS/IN2P3, F-33175 Gradignan Cedex, France*
[d] *CEA/DAM, DIF, Bruyeres-le-Chatel, F-91297 Arpajon Cedex, France*
[e] *LPC, ENSICAEN et Université de Caen, IN2P3/CNRS, F-14050 Caen cedex, France*
[f] *Institut de Physique Nucleaire, IN2P3-CNRS, F-91406 Orsay cedex, France*
[g] *Nuclear Physics Institute, AS CR, CZ-25068 Rez, Czech Republic*
[h] *Institute of Atomic Physics, IFIN-HH, Bucharest-Magurele, P.O. Box MG6, Romania*
[i] *CEA Saclay, DAPNIA/SphN, F-91191 Gif-sur-Yvette Cedex, France*
[j] *Helmholtz-Institut fur Strahlen- und Kernphysik, Universitat Bonn, Nussallee 14-16, D-53115 Bonn, Germany*
[k] *SUPA, School of Engineering, University of the West of Scotland, Paisley PA1 2BE, United Kingdom*
[l] *FLNR, JINR, 141980 Dubna, Moscow region, Russia*
[m] *IPHC, Université de Strasbourg, IN2P3/CNRS, BP28, F-67037 Strasbourg Cedex, France*
[n] *University of Surrey, GU2 7XH, United Kingdom*
[o] *Departamento de Física Teórica e IFT-UAM/CSIC, Universidad Autónoma de Madrid, E-28049 Madrid, Spain*

ARTICLE INFO

Article history:
Received 21 April 2011
Received in revised form 22 July 2011
Accepted 2 August 2011
Available online 9 August 2011
Editor: D.F. Geesaman

Keywords:
Nuclear structure
Knockout reactions
Shell closures
Neutron-rich Si nuclei

ABSTRACT

The structure of the very neutron-rich nuclei ^{39}Si and ^{41}Si has been investigated via in-beam γ-ray spectroscopy and few-nucleon knockout from radioactive beams. The observation of low-lying states in ^{39}Si is a clear evidence for a drastic lowering of the intruder neutron $3/2^-$ state when going from $Z = 20$ to $Z = 14$. The energy of the only γ-ray transition (672(14) keV) observed in ^{41}Si is significantly lower than that of the first excited state in ^{47}Ca (2014 keV) suggesting a deformed ground state for ^{41}Si. These results are consistent with large-scale shell-model calculations implying that strong proton–neutron correlations are the main reason for the lowering of the intruder configurations over the normal ones.

© 2011 Elsevier B.V. All rights reserved.

1. Introduction

The nuclei in the vicinity of the $N = 28$ shell closure offer a fertile ground for studying the various aspects of nuclear forces and correlations. The change in the single-particle energies as a function of the proton and neutron numbers leading to the reduction of the $N = 28$ shell gap below ^{48}Ca, as well as that in the splitting between the spin–orbit partners of the neutron $f_{7/2}$ and $p_{3/2}$ orbits, arises from the monopole terms of the nuclear interaction. In addition, correlations of a quadrupole character drive the development of a new "island of inversion" around ^{42}Si, where according to mean field [1] and shell-model [2–4] calculations, deformed intruder configurations fall below the spherical ones.

The development of the $N = 28$ island of inversion can be followed through the evolution in structure of the $N = 27$ isotones. In ^{45}Ar, a low-lying $3/2^-$ state has been observed at 537 keV above the $7/2^-$ ground state [5]. It has been shown via the ^{44}Ar(d, p) reaction that this state contains about half of the $p_{3/2}$ strength [3]. In ^{43}S, the ordering between the normal $7/2^-$ and the intruder $3/2^-$ states is changed. A low-energy $7/2^-$ isomer has been

* Corresponding author.
E-mail address: sohler@atomki.hu (D. Sohler).

0370-2693/$ – see front matter © 2011 Elsevier B.V. All rights reserved.
doi:10.1016/j.physletb.2011.08.004

discovered [6] connecting the $3/2^-$ ground state with a very low reduced transition probability B(E2). Based on the B(E2) and the measured g-factor, the $7/2^-$ isomeric state has been assigned to the $\nu f_{7/2}$ spherical configuration [7].

The observation of a deformed ground state [8] and a spherical isomeric 0^+ state [9] in ^{44}S confirms that it is within the island of inversion. From the low energy of the first excited state, ^{42}Si is also expected to have a deformed ground state [10]. The slight decrease of the 2^+ energy in ^{40}Si relative to the systematics was also invoked as an argument in favor of an enhanced collectivity [11].

To confirm that deformation is favored around $^{42}_{14}Si_{28}$ and to determine the location of the border of the island of inversion in the neutron-rich Si isotopes, we have studied the $^{39}_{14}Si_{25}$ and $^{41}_{14}Si_{27}$ isotopes, having 3 and 1 neutron–hole configurations with respect to an $N = 28$ core, respectively.

2. Experiment

Excited states in ^{39}Si and ^{41}Si were populated and studied in the present work via in-beam fragmentation of fast secondary beams. A ^{48}Ca beam of 60 MeV/u energy and 4 μAe intensity, delivered by the GANIL facility, was employed to bombard targets of ^{12}C and ^{181}Ta (~ 200 mg/cm^2). The secondary beams of interest were collected and selected using the SISSI device coupled to the α spectrometer in which a 50 μm Al achromatic degrader was placed between the two sets of dipole magnets. The magnetic rigidity ($B\rho$) was tuned to optimize the production of ^{40,41,42}P and ^{42,43,44}S for which average rates of 65, 130, 20, 120, 220 and 125 pps were obtained, respectively. A combination of energy-loss (ΔE) and time-of-flight information, measured using a 50 μm-thick Si and microchannel plate detectors, allowed unambiguous identification of the secondary beam particles on an event-by-event basis. Behind the Si detector a secondary Be target of 185 mg/cm^2 was used to induce secondary fragmentation.

The nuclei produced by the secondary fragmentation were selected using the SPEG spectrometer and identified by the ΔE, time-of-flight and $B\rho$. The ΔE was measured using an ionization chamber, while the time-of-flight was determined between the channel–plate detector located upstream of the target and a thick plastic-detector placed just behind the focal plane of the spectrometer. The $B\rho$ was inferred from the trajectories of the nuclei, which were obtained using two pairs of drift chambers straddling the focal plane. By combining the $B\rho$ and time-of-flight information, the mass-over-charge ratio can be derived to provide the identification matrix of the secondary fragments.

The ^{39}Si nuclei were produced by $1p$, $1p1n$, $2p1n$ and $2p2n$ knockout reactions from the ^{40,41}P and ^{42,43}S secondary beams, respectively. The production of ^{41}Si was almost equally shared between the $1p$, $2p$ and $2p1n$ reaction channels from ^{42}P, ^{43}S and ^{44}S. The $2p$ knockout cross section $^{43}\text{S} \rightarrow {}^{41}\text{Si}$ at 41.5A MeV was measured to be 71 ± 14 μbarn. This is comparable to the value of 80 ± 10 μbarn obtained for the $2p$ removal reaction $^{44}\text{S} \rightarrow {}^{42}\text{Si}$ [10].

The secondary target was surrounded by the 4π "Chateau de Crystal" array consisting of 74 BaF_2 scintillators to measure the emitted γ-rays. The individual detector threshold was set to about 100 keV. As the scintillators of the array were closely packed, an addback procedure was used to increase the photopeak efficiency leading to efficiencies of 38% at 779 keV and 24% at 1.33 MeV for fragments with $v/c \approx 0.3$. The γ-ray spectra were obtained by selecting, event-by-event, the nuclei of interest in the secondary beam and in SPEG following the interaction with the secondary target. Doppler corrections were applied based on the velocity of the ions as determined from the time-of-flight and trajectory information. The energy of the γ-ray lines used for the calibrations could be reproduced with a 6 keV uncertainty, which corresponds to the systematic uncertainty of the energy determination.

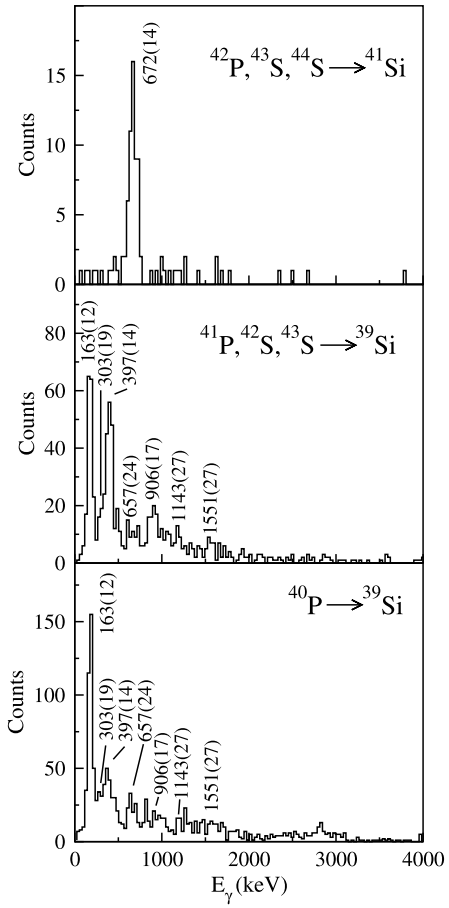

Fig. 1. γ-ray energy spectra obtained for ^{39}Si and ^{41}Si.

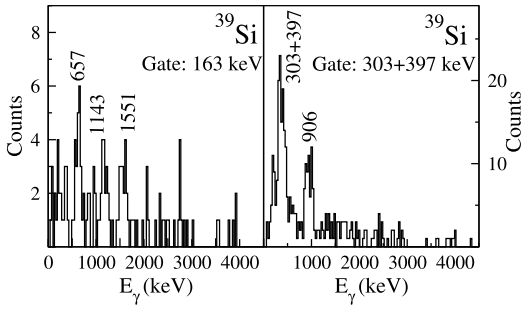

Fig. 2. γ-gated spectra for ^{39}Si using the 163 (left) and $303 + 397$ keV (right) transitions as gates.

3. Results

The γ-ray energy spectra for ^{39,41}Si are displayed in Fig. 1. In ^{41}Si, a clear peak is seen at 672 ± 14 keV. In the spectra for ^{39}Si, two strong γ transitions at 163 and 397 keV, as well as weaker ones at 303, 657, 906, 1143 and 1551 keV, were identified. The spectrum for ^{39}Si obtained using $1p$ knockout from ^{40}P is dominated by the 163 keV transition.

A $\gamma\gamma$-coincidence analysis was possible for ^{39}Si after adding together all the data from the various reaction channels. As shown in Fig. 2, the 163 keV transition is in coincidence with the 657, 1143 and 1551 keV ones, but not with the 397 keV transition. The two

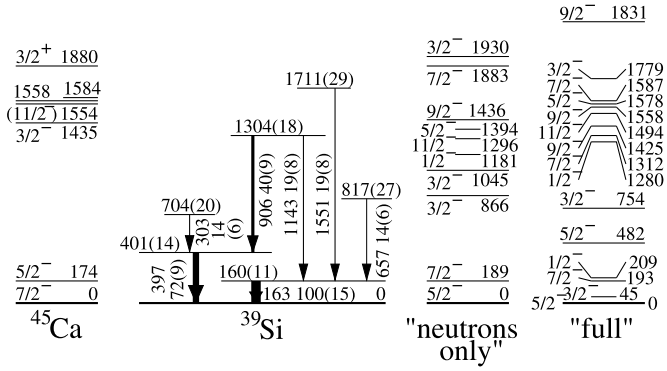

Fig. 3. Comparison of the experimental level schemes of the $N = 25$ isotones ^{39}Si and ^{45}Ca [18] with shell-model calculations for ^{39}Si assuming a closed proton core ("neutrons only"), and using the full valence sd–pf space ("full"). In the proposed level scheme for ^{39}Si the energies and relative intensities are listed with the uncertainties along the transitions. The width of the arrows is proportional to the intensity of the γ-rays.

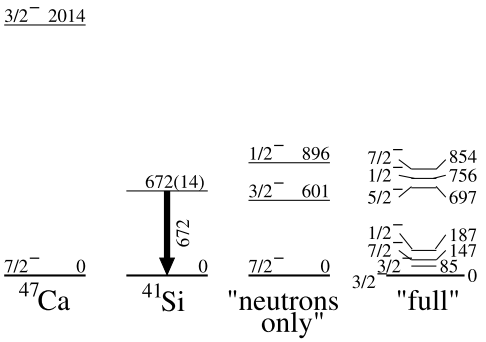

Fig. 4. Comparison of the experimental level schemes of the $N = 27$ isotones ^{41}Si and ^{47}Ca [15] with shell-model calculations of ^{41}Si assuming a closed proton core ("neutrons only"), and using the full valence sd–pf space ("full").

lines of the $303 + 397$ keV doublet are in mutual coincidence, and one or both of them are in coincidence with the 906 keV transition.

The level scheme of ^{39}Si displayed in Fig. 3 was constructed from the $\gamma\gamma$ coincidences, the relative intensities and the energy balance of the transitions. The energy of the excited states was determined using the fitting procedure of the Radware package [12] and the energies of the feeding and de-exciting γ lines, including uncertainties. As the most intense 163 and 397 keV γ-rays are not in coincidence, they are placed in parallel and directly connected to the ground state. The $397(14) + 906(17)$ and $163(12) + 1143(27)$ keV sum energies overlap with each other, within the experimental errors. Thus, they establish an excited state at 1304 keV. Although, the 303 keV transition is placed above the 401 keV state based on the $\gamma\gamma$ coincidences and the intensity argument, it cannot be excluded that this γ-ray feeds a higher-lying level. Based on the coincidence information, the 657 and 1551 keV transitions connect the levels at 817 and 1711 keV with the state at 160 keV, respectively.

4. Discussion

Given that the strengths of the $Z = 14$ (~5 MeV at $N = 28$ [13]) and $Z = 20$ (~5.3 MeV between $N = 22$ and 26 [14]) shell gaps are similar, it may be instructive to compare the spectra of the $^{39,41}_{14}$Si and $^{45,47}_{20}$Ca isotones.

The $7/2^-$ ground state of ^{47}Ca corresponds to a 1 neutron–hole configuration $f_{7/2}^{-1}$. The first excited state lies at 2.01 MeV excitation energy. This $3/2^-$ state has a rather pure 1 particle–2 hole configuration [15], being well populated in the ^{46}Ca(d, p) neutron stripping reaction [16] and extremely weakly populated in the ^{48}Ca(d, t) neutron pick-up reaction [17] owing to the closed shell structure of ^{48}Ca. In ^{41}Si, only a γ transition was identified, which we assign to the decay of a level at 672 keV (Fig. 4). This is significantly smaller than the energy of the first excited state in ^{47}Ca, indicating that the two nuclei have very different structure. The low energy of the state at 672 keV in ^{41}Si suggests a deformed configuration, as for the neighboring nucleus ^{42}Si which has a low-lying 2_1^+ state [10].

The low-energy structure of ^{45}Ca can be described by 3 neutron–hole configurations with respect to a ^{48}Ca core. This leads to a multiplet of states based on the $f_{7/2}^{-3}$ configuration: the two first states – the $7/2^-$ ground state and the $5/2^-$ first excited state – are separated by only 174 keV, while the other members of the multiplet are found above 1.43 MeV [18]. In ^{39}Si, the ground and the first excited states are separated by 160 keV and may also arise from the neutron $f_{7/2}^{-3}$ configuration. However, the existence of other low-lying states in ^{39}Si reveals a structural change relative to ^{45}Ca and indicates the presence of low-lying intruder configurations already at $N = 25$.

These results point to a significant change in nuclear structure between the Ca and the Si isotopic chains. This feature could be accounted for by the decrease in size of the $N = 28$ shell gap by about 1 MeV in the Si nuclei compared to the corresponding Ca isotones, as it has been shown both for $N = 20$ [19] and 28 [20]. For instance, the $N = 28$ gap of ~4.5 MeV in ^{48}Ca [14] is estimated to decrease to ~3.5 MeV in ^{42}Si [20]. Thus, it may be assumed that the decreasing $N = 28$ shell gap is responsible for the lowering of the intruder configurations observed.

To verify this hypothesis, shell-model calculations were carried out using the SDPF-U interaction [2] with a closed proton $Z = 14$ core and the neutron fp-valence space. These calculations are labeled "neutrons only" in Figs. 3 and 4. As it may be seen in the level schemes reported in Fig. 3, the low-energy structure of ^{39}Si is not fully reproduced by these calculations which rather predict a spectrum similar to that of ^{45}Ca, but more compressed in energy. Only two low-lying states are calculated, together with a high-density region of levels starting at 866 keV. The latter occurs lower in energy compared to ^{45}Ca in line with the decrease in energy of the 2^+ states in the Si isotopes relative to Ca. These calculations suggest that the decrease in the $N = 28$ shell gap alone cannot explain the lowering of the intruder states. By inhibiting proton excitations, there is not enough degree of freedom to account for the observed experimental spectrum.

To investigate the role of the proton excitations across the $Z = 14$ gap, the level schemes for ^{39,41}Si were recalculated using the full sd proton and fp neutron valence space reported as "full" in Figs. 3 and 4. Comparing the results of these calculations to the experiment, the low-energy level scheme of ^{39}Si is better reproduced by the full space calculations which predict a $\nu f_{7/2}^{-3}$ $5/2^-$ ground state and low-lying $7/2^-$ and $3/2^-$ states with strong $\nu f_{7/2}$ and $\nu p_{3/2}$ components. The decay of the first two excited states in ^{39}Si is consistent with this picture. In addition, the calculated level density is also consistent with the experimental one. In ^{41}Si, two groups of low-lying states, centered around 750 keV and 150 keV, are predicted by the "full" shell-model calculations. These groups are separated by about 600 keV, which is close to the energy of the observed peak in the γ-ray spectrum at 672 keV. Note that, given its energy width, this line may correspond to a multiplet. The observation of γ lines from the lowest energy group of states is hampered for two reasons. First, they lie

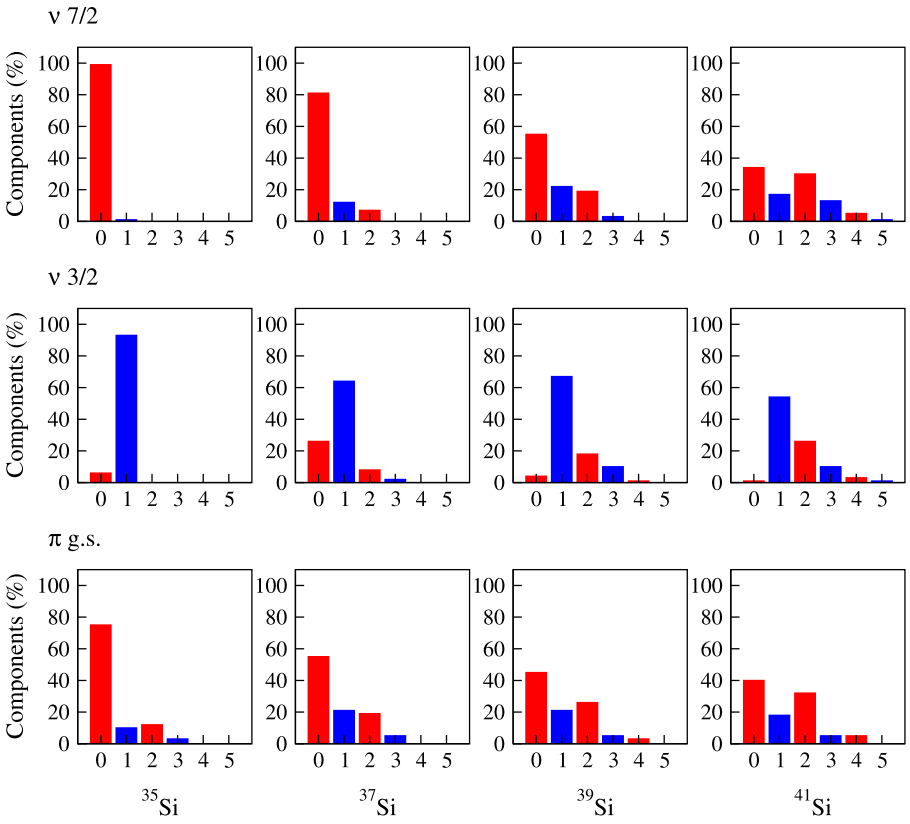

Fig. 5. Contributions of the neutron cross shell excitations to the $7/2^-_1$ (top), $3/2^-_1$ (middle) states and proton cross shell excitations (bottom) to the ground state wave functions of odd Si isotopes between $N = 20$ and 28. On the x axis the number of excitations with respect to the $\nu f_{7/2}$ and the $\pi d_{5/2}$ orbits are indicated.

below the 150 keV threshold of the gamma-array. Second the $7/2_1$ state in ^{41}Si, built principally on the $\nu f_{7/2}$ orbit, is predicted to be an isomeric state with a half-life of about 400 ns similar to ^{43}S [6,7]. Such a decay could not be observed here where only prompt γ-rays were detected. The "full" shell-model calculations, which predict a low-lying intruder $3/2^-$ state in ^{39}Si and a $3/2^-$ ground state for ^{41}Si, suggest that the order of the normal $7/2^-$ and the intruder $3/2^-$ states inverts between $A = 39$ and 41.

To better identify the respective contributions of the proton and neutron excitations to the onset of collectivity while approaching $N = 28$, the shell-model wave functions of the "normal" $7/2_1$ and the "intruder" $3/2_1$ states were analyzed in the heavy odd Si nuclei. As it may be seen in Fig. 5, near $N = 20$ *both* the $7/2^-_1$ and the $3/2^-_1$ states exhibit clear neutron single-particle characters. Indeed, the wave functions correspond mainly (more than 85%) to 0-particle–0-hole and 1-particle–1-hole configurations, respectively. Conversely, when approaching $N = 28$, the amount of cross-shell excitations, i.e. the collectivity of the states, gradually increases in *both* the "normal" and "intruder" states. Despite the fact that the $N = 28$ shell gap *increases* by about 0.8 MeV per pair of neutrons added between $N = 20$ and 28 [14], deformation develops as if $N = 28$ was at mid-shell. As it is shown in Fig. 5, the role of proton and neutron cross shell excitations in the shell-model calculations increases with increasing mass, being a maximum for the ground state of ^{41}Si. Experimentally, the lowering of the intruder states is indicated by the increasing complexity of the level schemes of the odd Si nuclei with increasing mass number. The gradual increase of the ground state deformation has been revealed by (p, p') studies of the even–even Si nuclei [21].

To obtain a better understanding of which type of correlations induce the deformation at $N = 28$ in the Si chain, Fig. 6 presents the correlation energy of the $7/2^-_1$ state calculated using three different valence spaces: "neutrons only" in which the proton core is frozen; "$N = 28$ closed" in which the neutrons are frozen in the $f_{7/2}$ orbit, and "full" in which both protons and neutrons can be excited. From the "neutrons only" calculations, the contribution of the neutron–neutron correlations slowly increases with increasing mass number but saturates at $N = 28$. Calculations for the "$N = 28$ closed" case exhibit a single closed shell behavior with an increased correlation at the mid-shell. These two calculations are consistent with $N = 20$ and 28 shell closures. The role of the cross-shell proton–neutron excitations can be deduced from the "full" calculations. These exhibit a steady increase of the correlations up to 15.8 MeV, rather than a saturation at $N = 27$. By comparing this to the estimated size of the $N = 28$ spherical gap of 3.5 MeV, up to 5-particle–5-hole configurations are possible, again suggesting that the nuclei around $N = 28$ rather behave as if they were at mid-shell. This observation may be connected with the fact that

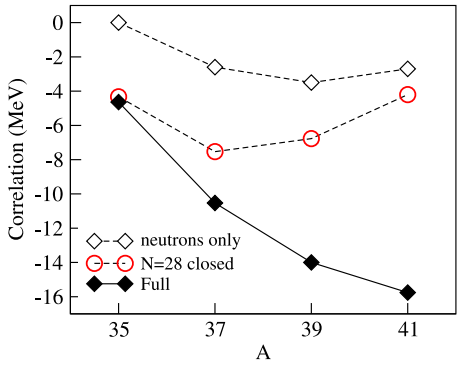

Fig. 6. Correlation energies calculated for the $7/2^-_1$ state in the Si isotopes. Lines are to guide the eye.

both the $N = 28$ and $Z = 14$ shell gaps occur within a major shell, i.e. the *sd* shell for protons and the *fp* shell for neutrons. As a consequence, 1-particle–1-hole quadrupole cross-shell excitations can also take place, which limit the energy required for cross-shell excitations in spite of there being relatively large shell gaps. In addition, the "normal" and "intruder" configurations have the same parity, which allows for mixing of the normal and cross-shell excitations resulting in deformation of the normal states, as well. Similar mechanism might dictate the energy of the intruder states in ^{78}Ni, where both the $Z = 28$ and the $N = 50$ shell gaps separate states from the same major *fp* and *gds* oscillator shells, respectively. This mechanism differs significantly from the development of island of inversion at $N = 8$ or $N = 20$, where the cross-shell excitations take place between different oscillator shells having different parity.

5. Summary

Excited states in ^{39}Si and ^{41}Si have been identified for the first time. A comparison of the level structure of ^{39,41}Si with that of the ^{45,47}Ca isotones, as well as with the results of large-scale shell-model calculations, was used to infer the lowering of the intruder states in ^{39,41}Si. A low-lying intruder state in ^{39}Si and a deformed ^{41}Si ground state are proposed. Based on the shell-model calculations, it is suggested that the border of the $N = 28$ island of inversion falls between $N = 25$ and 27 in the Si isotopes, confirming that ^{42}Si lies in a region of deformation. It is shown that to account for the low-lying level structure of ^{39,41}Si, both neutron *and* proton excitations across the $N = 28$ and $Z = 14$ shell closures are required.

Acknowledgements

The authors wish to thank the staff from GANIL and LPC for their assistance in preparing and executing the experiment. This work has partially been supported by the EC through the Eurons contract RII3-CT-3/2004-506065, OTKA K68801, TéT FR-9/2009, BMBF 06BN109, Czech Republic GA 202/040791, the "Dubna-IN2P3" Agreement, grant RFFI-09-02-91056 and by the Bolyai János Foundation. AP's work is partly supported by a grant of the Spanish Ministry of Education and Science (FPA2009-13377) and by the Comunidad de Madrid (Spain), project HEPHACOS S2009/ESP-1473. FN and AP's work is partly supported by the IN2P3(France)-CICyT(Spain) collaboration agreement.

References

[1] T.R. Werner, et al., Nucl. Phys. A 597 (1996) 327;
P.-G. Reinhardt, et al., Phys. Rev. C 60 (1999) 014316;
G.A. Lalazissis, et al., Phys. Rev. C 60 (1999) 014310;
S. Péru, et al., Eur. Phys. J. A 9 (2000) 35;
R. Rodriguez-Guzman, et al., Phys. Rev. C 65 (2002) 024304.
[2] F. Nowacki, A. Poves, Phys. Rev. C 79 (2009) 014310.
[3] L. Gaudefroy, et al., Phys. Rev. C 78 (2008) 034307.
[4] L. Gaudefroy, Phys. Rev. C 81 (2010) 064329.
[5] Zs. Dombrádi, et al., Nucl. Phys. A 727 (2003) 195.
[6] F. Sarazin, et al., Phys. Rev. Lett. 84 (2000) 5062.
[7] L. Gaudefroy, et al., Phys. Rev. Lett. 102 (2009) 092501.
[8] T. Glasmacher, et al., Phys. Lett. B 395 (1997) 163.
[9] C. Force, et al., Phys. Rev. Lett. 105 (2010) 102501.
[10] B. Bastin, et al., Phys. Rev. Lett. 99 (2007) 022503;
B. Bastin, PhD thesis, Université de Caen, LPCCT 07-03, http://tel.archives-ouvertes.fr/docs/00/26/98/86/PDF/these_bastin.pdf.
[11] P.M. Campbell, et al., Phys. Rev. Lett. 97 (2006) 112501.
[12] D.C. Radford, Nucl. Instrum. Methods A 361 (1995) 297.
[13] P.D. Cottle, K.W. Kemper, Phys. Rev. C 58 (1998) 3761.
[14] O. Sorlin, M.G. Porquet, Prog. Part. Nucl. Phys. 61 (2008) 602.
[15] T.W. Burrows, Nuclear Data Sheets 108 (2007) 923.
[16] T.A. Belote, et al., Phys. Rev. 142 (1966) 624.
[17] M.E. Williams-Norton, Nucl. Phys. A 291 (1977) 429.
[18] T.W. Burrows, Nuclear Data Sheets 109 (2008) 171.
[19] S. Nummela, et al., Phys. Rev. C 63 (2001) 044316.
[20] L. Gaudefroy, et al., Phys. Rev. Lett. 97 (2006) 092501.
[21] P.M. Campbell, et al., Phys. Lett. B 652 (2007) 169.